Direct Evidence of Catalytic Heterogeneity in Lactate Dehydrogenase by Temperature Jump Infrared Spectroscopy

*Michael Reddish,[$] Huo-Lei Peng,[‡] Hua Deng,[‡] Kunal S. Panwar,[$], Robert Callender[‡], and R. Brian Dyer[$]**

[$]Department of Chemistry, Emory University, Atlanta, GA 30322

[‡]Department of Biochemistry, Albert Einstein College of Medicine, Bronx, NY 10461

* Phone: 404-727-6637, Fax: 404-727-6586, E-mail: briandyer@emory.edu

Supplemental Material

Explanation of Kinetic Modeling

We compare the calculated relaxation kinetics of various kinetic systems with the experimental results and score similarity. To determine equilibrium concentrations of all states at each temperature, we used a master equation approach. Namely, equilibrium concentrations were calculated in a stepwise fashion for a large number of time steps till changes in concentration became insignificant ($\sim e^{-10}$).

Calculating the relaxation transients requires computing relaxation times and amplitudes. There are multiple approaches to calculating these values and some are cited here for the interested reader.[1-5] The approach we used was informed by the method of Bernasconi and is based on an eigenvalue decomposition.[6] Below we present a trivial example of the approach we used. In reality, the 12 different reaction steps of our model (see Scheme S3 below) requires a much more complex version of this method utilizing all 22 relevant rate constants. The system can be minimized, but still leads to a matrix for step S.8 that is 10 by 10. Consider the simple scheme:

$$A + B \underset{k_{-1}}{\overset{k_1}{\leftrightarrow}} C \underset{k_{-2}}{\overset{k_2}{\leftrightarrow}} D \tag{S.1}$$

whose differential rate equations can be written in terms of the change in concentration with time and simplified into two expressions which fully describe the system:

$$\frac{d\Delta A}{dt} = -\left[k_1(A_{eq} + B_{eq} + k_{-1}\right]\Delta A - k_{-1}\Delta D \tag{S.2}$$

$$\frac{d\Delta D}{dt} = -k_2\Delta A - (k_2 + k_{-2})\Delta D \tag{S.3}$$

Where ΔX stands for the change in concentration of a state and X_{eq} is the concentration of a state at equilibrium. Equations S.2 and S.3 form a system of coupled differential equations that have a solution of the general form:

$$x_1 = x_1^{01}\exp\left(-t/\tau_1\right) + x_1^{02}\exp\left(-t/\tau_2\right) \tag{S.4}$$

$$x_2 = x_2^{01}\exp\left(-t/\tau_1\right) + x_2^{02}\exp\left(-t/\tau_2\right) \tag{S.5}$$

We can solve for the constants x_1^{01}, x_1^{02}, x_2^{01}, x_2^{02}, τ_1, and τ_2 by using a standard eigenvalue decomposition:

$$\vec{X} = [A]\vec{x} \tag{S.6}$$

$$\text{where } \vec{X} = \begin{bmatrix} \frac{d\Delta A}{dt} \\ \frac{d\Delta D}{dt} \end{bmatrix}, \tag{S.7}$$

$$[A] = \begin{bmatrix} -[k_1(A_{eq} + B_{eq} + k_{-1}] & -k_{-1} \\ -k_2 & -(k_2 + k_{-2}) \end{bmatrix}, \tag{S.8}$$

$$\text{and } \vec{x} = \begin{bmatrix} \Delta A \\ \Delta D \end{bmatrix} \tag{S.9}$$

The eigenvalues to the above problem correspond to relaxation rates (τ in equation S.4), and eigenvectors, which transform into the relaxation amplitudes (x_1^{01}, x_1^{02}, etc.). Theoretical transients for a system are then generated using equations S.4 and S.5 where each equation yields the time-dependent change in concentration of a state of the reaction. The similarity between the theoretical and experimental result is presented as a score value (perfect match is zero). The scoring method considers all five of the transients collected at different probe frequencies. First, we calculate an accuracy score for each transient as shown in equation S.10.

$$Score_j = \sum_i^n \left(experimental_i - predicted_i\right)^2 \tag{S.10}$$

Where *j* is each wavenumber, *n* is the total number of points in the transient, and *i* is a given point in time. This method gives a direct measure of how accurately the predicted transient matches the experiment and ignores whether the predicted data over- or under-estimates the experimental data. Finally, a composite score for an entire fitting run is compiled as the summation of all the transient scores as shown in equation S.11.

$$Total\ Score = \sum_j\ Score_j \tag{S.11}$$

The total score is used for comparison between simulation and experiment. The entire process is then cycled in a Monte Carlo fashion where one randomly chosen rate constant is modified; the transients are recomputed and scored. If the modified rate constant results in a better score, signifying a progress, then the modification is saved and repeated. If the

modification results in a worse score, then the change is discarded and the procedure restarts. The Monte Carlo simulations are run many times to find the optimum rate constant set for a given kinetics model.

We also worked with a few modifications of the main routine outlined above. In addition to inputting a guess set of rate constants for a given kinetics model, we ran calculations where we used the random number generator in MATLAB to generate random starting points for the Monte Carlo simulations. The allowed values for these random start points were constrained to be within an order of magnitude of the values provided by Zhadin.[7] Using random start rate constants allowed us to make sure that the score values we were calculating were not local-minimum, or trap, solutions to the problem, but were in fact the overall lowest scores possible. When we performed calculations allowing the activation energies of the system to change as well, we simply added the activation energies relevant to the competent encounter complex as possible values to be altered in the Monte Carlo process. Of course, if a change in these values led to a worse score, those values were discarded.

Reaction Schemes

There have been a number studies concerning the kinetic pathway of Michaelis complex formation; the pig heart LDH isozyme is the best studied. An excellent mimic of the substrate pyruvate is oxamate ($NH_2(C_2{=}O)COO^-$), and the binding kinetics of this to LDH•NADH can be studied without consideration of any chemical event. The results are useful in guiding a kinetic model of the Michaelis complex formed with actual substrate.

The following kinetic scheme fully describes the available data[8-10]:

Scheme S1

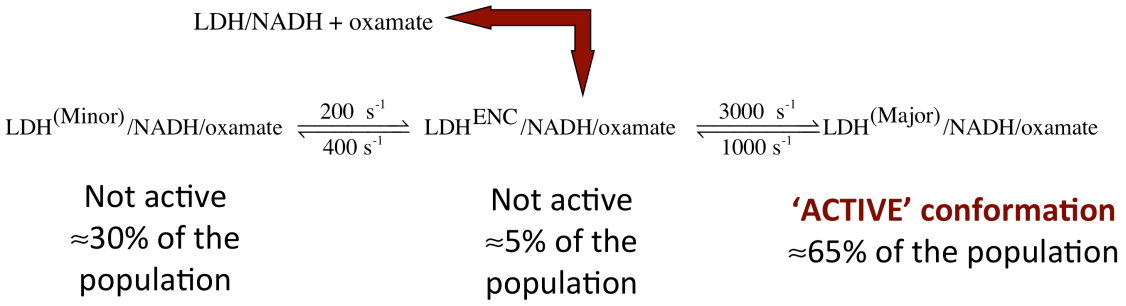

The two well-populated ternary complexes are observed directly by characteristic C2=O stretch IR bands, which indicate the strength of the hydrogen bonds between the C2=O moiety and polar active site residues (see Figure 1). In addition to the sub-millisecond kinetics associated with changing hydrogen bond conformations, sub-millisecond kinetics of the movement of atoms within the protein are also observed.[11] These two populated conformations are inferred to have differing propensities towards chemistry (denoted as 'active' or 'not active') by the positions of the observed IR bands as well as characteristic C4-D stretch positions of NADH bound in the two observed populated LDH•NADH•oxamate conformations[12-13]. The two populated conformations do not interconvert directly but rather through another weakly populated state or states (labeled as an encounter complex).

Previous to the current study, the best worked out reaction scheme for the binding of pyruvate to LDH•NADH to the formation of LDH•NAD^+ plus lactate is based on the T-jump optical absorption and emission study of Zhadin et al.[7]

Scheme S2

$$\text{LDH•NADH} + \text{py} \rightleftharpoons \text{LDH•NADH•py}^{open} \rightleftharpoons$$

$$\text{LDH•NADH•py}^{closed} \xrightleftharpoons{chemistry}$$

where LDH•NADH•py^{open} denotes a loosely bound pyruvate molecule typically assumed with a catalytically critical LDH surface loop (residues 98-110) in an 'open' conformation. Loop closure is believed to be the rate limiting step of on-enzyme hydride transfer. The kinetics modeling routine we wrote was given starting concentrations and temperatures that matched the experiments, and initially was given rate constants for the final temperature of the jump and activation energies that matched the work of Zhadin et al.[7] The activation energies were used to estimate the lower temperature rate constants in an Arrhenius fashion.

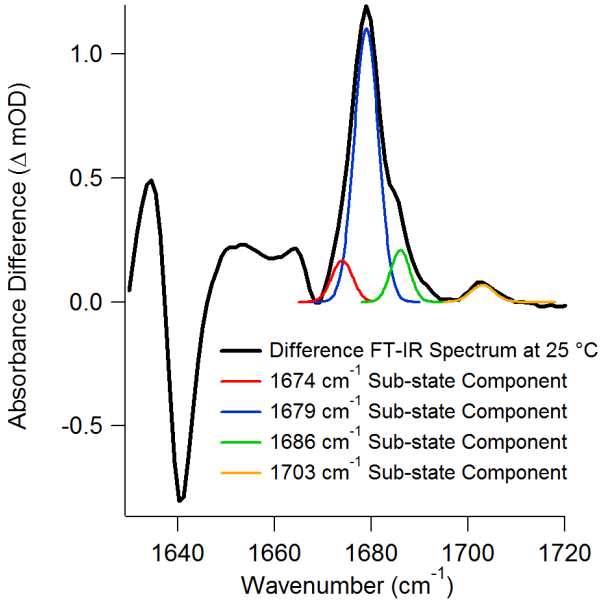

Figure S1: The IR difference spectrum in the spectral region for pyruvate in [U-^{15}N, -^{13}C]LDH•NADH•[2-^{12}C]pyruvate - [U-^{15}N, -^{13}C]LDH•NADH•[2-^{13}C]pyruvate. Gaussian deconvolution fits are shown with peaks at 1674, 1679, 1686, and 1703 cm^{-1}.[11] This image also shows the negative [2-^{13}C]pyruvate carbonyl main peak at 1641 cm^{-1} and the minor peak is obscured but visible at 1660 cm^{-1}.

Figure S1 shows the isotope edited IR spectrum of pyruvate's C2=O moiety within the phLDH•NADH•pyruvate ternary complex.[14] The isotope edited IR results indicate that at least several 'closed' states must be included in any kinetic scheme: LDH•NADH•pruvate^{1686}, LDH•NADH•pruvate^{1679}, and LDH•NADH•pruvate^{1674}."

Analysis of Probe Frequencies and Contribution of Individual Sub-states

We used the fitting parameters from reference 11 to reproduce the component Gaussian peaks that make up the equilibrium FT-IR difference spectrum as shown above in Figure S1. By using a simple calculation of the contribution of a given Gaussian divided by the total Gaussian signal, we can estimate the contribution of a sub-state at a given probe frequency (see equation S.12).

$$\text{Contribution of Sub-State fit } f_i(\text{j}) \text{ to Signal at Frequency } j = \frac{f_i(j)}{\sum_i f_i(j)} \qquad \text{(S.12)}$$

This analysis indicates that a single sub-state is dominant at each of our chosen probe frequencies. Each column of Table S1 shows that for the corresponding probe frequency a single sub-state contributes at least 75 % or more of the observed IR absorbance.

Table S1: Contribution of Each Sub-state to a Given Frequency

	Probe at 1670 cm^{-1}	Probe at 1679 cm^{-1}	Probe at 1685 cm^{-1}	Probe at 1704 cm^{-1}
Contribution of 1674 cm^{-1} Population	0.95	0.01	0	0
Contribution of 1679 cm^{-1} Population	0.05	0.99	0.25	0
Contribution of 1686 cm^{-1} Population	0	0	0.75	0
Contribution of 1703 cm^{-1} Population	0	0	0	1

List of Reaction Schemes Tested

Original Scheme

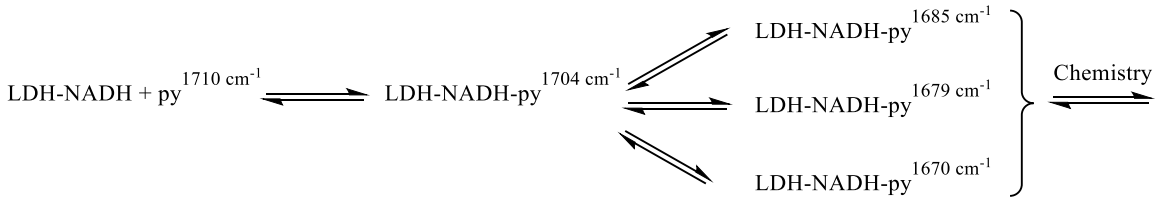

Extra Michaelis State

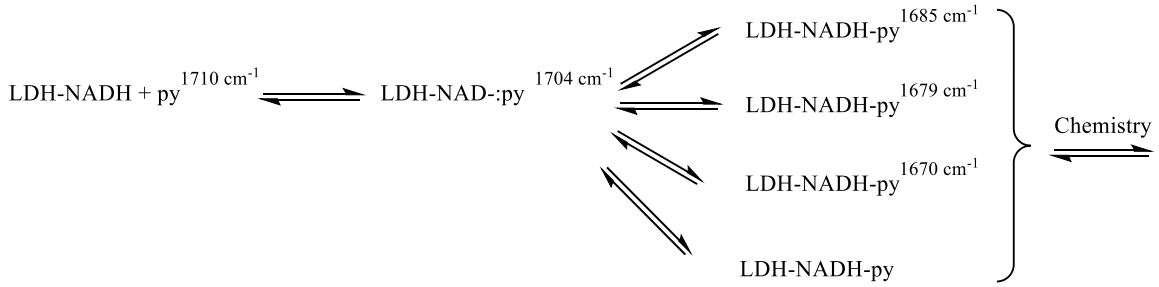

Michaelis Dead End State

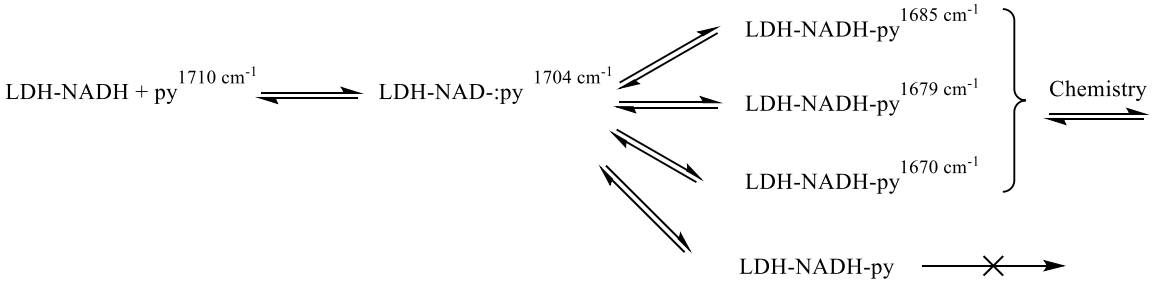

Additional Encounter Complex that Do Not Go On to tightly bound conformations

Models where the 1704 cm^{-1} IR band was assigned to both encounter complexes or just one were separately tried.

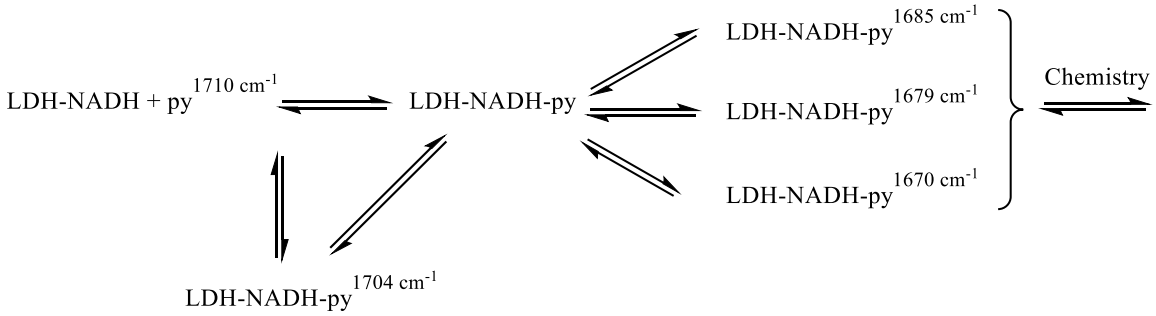

Best Scheme, Additional Dead-End Encounter Complex

Models where the 1704 cm^{-1} IR band was assigned to both encounter complexes or just one were separately tried.

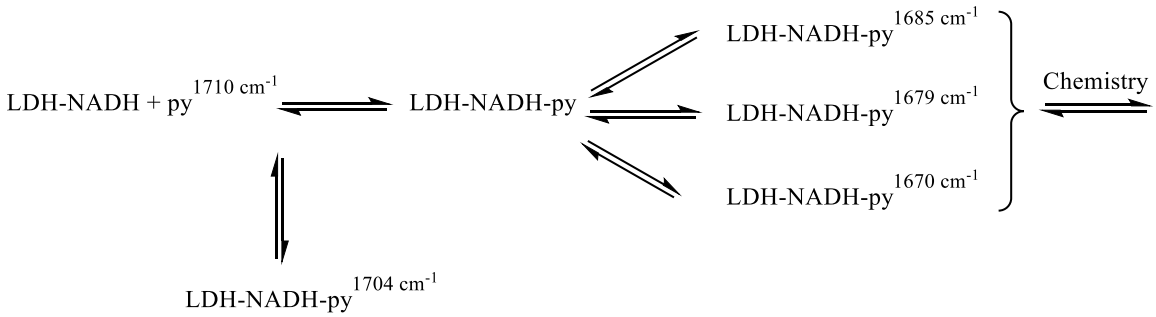

Kinetic Parameters of Solutions Shown in Figure 4

We present below the solutions that were generated from our modeling routine for the rate constants used to generate the solutions shown in the main text of the article. The reaction schemes shown in the article and above do not display all the reaction steps included in the calculations. This was done for simplicity. Below we display a reaction scheme showing all the reactions steps considered in the calculations.

Scheme S3

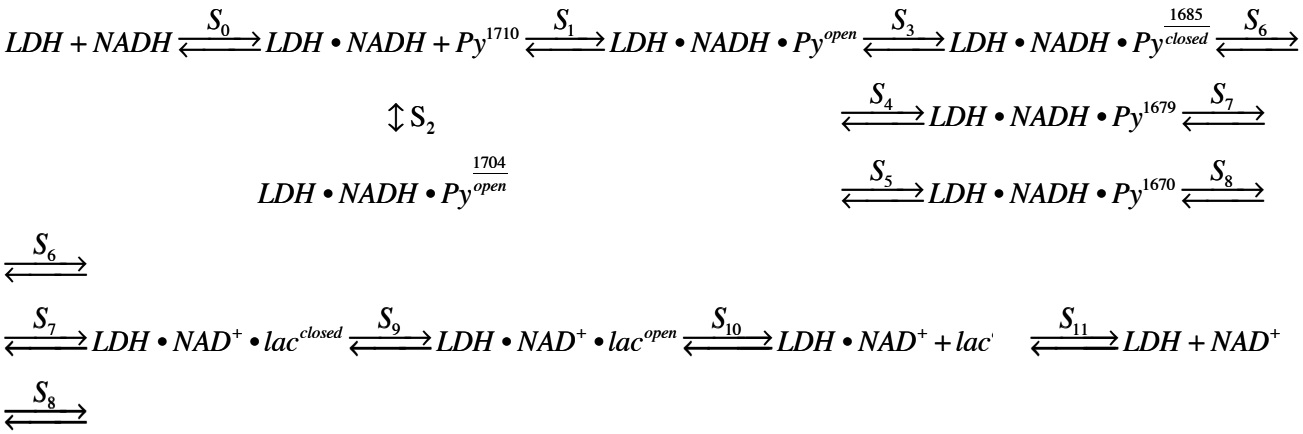

Table S2: Kinetic Parameters of Solutions Shown in Main Text

Mechanism Step	Figure 4A Rate Constants ($M^{-1}s^{-1}$ or s^{-1} as appropriate)[a]	Figure 4A ΔG‡ (J/mol)[b]	Figure 4B Rate Constants ($M^{-1}s^{-1}$ or s^{-1} as appropriate)[a]	Figure 4B ΔG‡ (J/mol)[b]
S_0	5.6×10^7	41400	5.0×10^7	41400
S_{-0}	75	81170	75	81170
S_1	2.0×10^7	23800	5.0×10^7	23800
S_{-1}	1750	67360	1500	67360
S_2	N/A	N/A	1.4×10^8	100000
S_{-2}	N/A	N/A	3100	33000
S_3	6100	10900	9.5	10900
S_{-3}	21	-10500	75	-10500
S_4	57	10900	3200	10900
S_{-4}	99	-10500	330	-10500

S_5	6200	10900	11000	10900
S_{-5}	20	-10500	3500	-10500
S_6	4300	58990	4000	58990
S_{-6}	100	52300	290	52300
S_7	4300	58990	7900	58990
S_{-7}	490	52300	700	52300
S_8	38000	58990	16000	58990
S_{-8}	690	52300	9.5	52300
S_9	470	61500	470	61500
S_{-9}	940	61920	940	61920
S_{10}	1.2×10^5	8368	1.1×10^5	8368
S_{-10}	3.0×10^7	1130	3.0×10^7	1130
S_{11}	560	8790	540	8790
S_{-11}	6.2×10^7	5020	6.1×10^6	5020

[a] Values were rounded to 2 significant figures for clarity.

[b] Values are presented as what was used in calculations.

Estimation of k_{cat} for Our Model

To estimate k_{cat} for the model presented in Scheme 2 of the main paper with the kinetic parameters listed in Table S2 above we modified the master equation program discussed above for the theoretical studies for analysis of the system by the method of initial rates. The concentration of phLDH (1 nM) and NADH (100 mM) was kept constant while the concentration of pyruvate was varied. The time-dependent change in lactate concentration was

recorded and an initial rate was fit for each pyruvate concentration. The data was then plotted and fit in the Lineweaver-Burke method to determine k_{cat}. Figure S2 below summarizes these results.

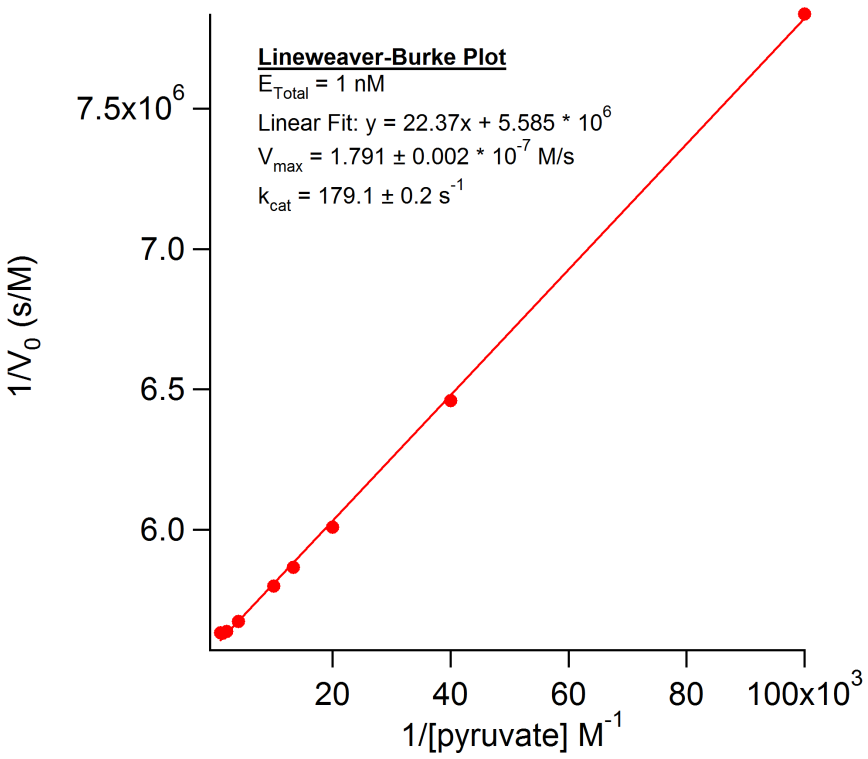

Figure S2: Lineweaver-Burke plot to determine k_{cat} of our proposed model.

References

1. Eigen, M.; Demaeyer, L., In *Techniques of Chemistry*, Hammes, G. G., Ed. Wiley (Interscience): New York, 1973; Vol. VI, p 63.
2. Eigen, M.; DeMaeyer, L., In *Technique of Organic Chemistry*, Friess, S. L.; Lewis, E. S.; Weissberger, A., Eds. Wiley (Interscience): New York, 1963; Vol. VIII, p 895.
3. Kustin, K.; Shear, D.; Kleitman, D., Theory of Relaxation Spectra; the Kinetics of Coupled Chemical Reactions. *J. Theor. Biol.* **1965,** *9* (2), 186-212.
4. Hayman, H. J. G., Orthonormal Chemical Reactions and Chemical Relaxation .2. Reactions in Non-Ideal Solutions. *Transactions of the Faraday Society* **1970,** *66* (570), 1402-&.
5. Schwarz, G., Kinetic Analysis by Chemical Relaxation Methods. *Reviews of Modern Physics* **1968,** *40* (1), 206-&.
6. Bernasconi, C. F., *Relaxation Kinetics*. Academic Press: New York, 1976; p xi, 288 p.
7. Zhadin, N.; Gulotta, M.; Callender, R., Probing the Role of Dynamics in Hydride Transfer Catalyzed by Lactate Dehydrogenase. *Biophys. J.* **2008,** *95* (4), 1974-1984.
8. McClendon, S.; Vu, D.; Clinch, K.; Callender, R.; Dyer, R. B., Structural Transformations in the Dynamics of Michaelis Complex Formation in Lactate Dehydrogenase. *Biophysical J.* **2005,** *89*, L07-L09.
9. McClendon, S.; Zhadin, N.; Callender, R., The Approach to the Michaelis Complex in Lactate Dehydrogenase: The Substrate Binding Pathway. *Biophysical J.* **2005,** *89*, 2024-2032.
10. Deng, H.; Brewer, S. H.; Vu, D. V.; Clinch, K.; Callender, R.; Dyer, R. B., On the Pathway of Forming Enzymatically Productive Ligand-Protein Complexes in Lactate Dehydrogenase. *Biophys. J.* **2008,** *95*, 804-813.
11. Peng, H.-L.; Deng, H.; Dyer, R. B.; Callender, R., Energy Landscape of the Michaelis Complex of Lactate Dehydrogenase: Relationship to Catalytic Mechanism. *Biochemistry* **2014,** *53* (11), 1849-1857.
12. Chen, Y.-Q.; van Beek, J.; Deng, H.; Burgner, J.; Callender, R., Vibrational Structure of Nad(P) Cofactors Bound to Several Nad(P)-Linked Enzymes: An Investigation of Ground State Activation. *J. Phys. Chem.* **2002,** *106*, 10733-10740.
13. Qiu, L.; Gulotta, M.; Callender, R., Lactate Dehydrogenase Undergoes a Substantial Structural Change to Bind Its Substrate. *Biophysical J.* **2007,** *93*, 1677-1686.
14. Peng, H.-L.; Deng, H.; Dyer, R. B.; Callender, R., The Energy Landscape of the Michaelis Complex of Lactate Dehydrogenase: Relationship to Catalytic Mechanism. *Biochemistry* **2014**, *53*, 1849-1857.